International Journal of Industrial Electronics, Control and Optimization © 2021 IECO
Vol. 4, No. 1, pp. 13-22, Jan (2021)

Adaptive Robust Tracking Control Based on Backstepping Method for Uncertain Robotic Manipulators Including Motor Dynamics

Javad Keighobadi[1†], Mohammad Mehdi Fateh[2]

[1,2] Department of Electrical and Robotic Engineering, Shahrood University of Technology, Shahrood, Iran

ABSTRACT

Recent research on the backstepping control of robotic systems has motivated us to design a robust backstepping voltage-based controller with computational simplicity and ease of implementation. In this paper, an adaptive robust tracking controller based on backstepping method (ARTB) is presented for uncertain electrically-driven robotic manipulators in the framework of voltage control strategy. It is intended to convert robot control problem to motor control problem. In the design procedure, the manipulator dynamics are incorporated into a lumped uncertainty, such that the proposed adaptation law promptly compensates for it. Hence, high tracking accuracy, robust behavior and less complexity are the prominent features of the proposed control system in the presence of external disturbances, parametric uncertainties and un-modeled dynamics. The stability of the closed-loop system is guaranteed based on the Lyapunov theory and the tracking error converges to zero asymptotically. As a case study, the proposed ARTB is simulated on a two-link robot manipulator driven by permanent magnet DC motors. Numerical simulations are included to show the superiority of the proposed controller to a state augmented adaptive backstepping method, a sliding backstepping controller and an adaptive backstepping sliding mode control in tracking the desired trajectory.

Article Info

Keywords:
Adaptation Mechanism, Backstepping Method,
Electrically-driven Robotic Manipulators, Robust Tracking Control,
Voltage-based Control

Article History:
Received 2019-09-29
Accepted 2020-04-28

I. INTRODUCTION

Robotic manipulators play an important role in many applications; hence, tracking purpose is a significant and challenging issue in robotics. As a result, numerous control techniques have been reported in the literature to achieve proper tracking of robotic systems in the presence of uncertainties [1]–[4]. In [5], a neuro fuzzy sliding mode control was proposed for a two-link robot manipulator, in which the parameters of sliding surface were optimized using PSO algorithm. Yin et al. [6] developed an adaptive robust tracking controller for an industrial robot such that the parametric estimation errors were compensated for through the projection-type adaptation mechanism. Yovchev et al. [7] suggested an iterative learning method to control the motion of the robot arm in a constrained state space in the presence of uncertainties. In [8], velocity and disturbance observers were designed to construct a tracking controller for uncertain robot manipulators.

Among the control approaches, the backstepping method is a powerful systematic Lyapunov-based control scheme which solves the regulation and tracking control problems of nonlinear strict-feedback systems [9]–[12]. To achieve high-accuracy tracking and extend the applicability of the backstepping method for robotic systems, it has been combined with other techniques as clearly reported in the literature. In [13], an adaptive backstepping control based on state augmentation was designed for a robotic manipulator. Nikdel et al. [14] proposed a fractional-order adaptive backstepping control for robotic systems in the presence of uncertainties. A fuzzy backstepping approach was proposed for robot manipulators using the funnel control technique [15].

[†]**Corresponding Author**: javad_keighobadi@yahoo.com
Department of Electrical and Robotic Engineering, Shahrood University of Technology, Shahrood, Iran

In [16], a PID fuzzy backstepping algorithm was presented to control the flexible-joint robot manipulator. Vijay et al. [17] suggested an observer-based backstepping terminal sliding mode control for robot manipulator, so that a neural network system was employed to approximate the unknown terms. In [18], an adaptive fuzzy backstepping control was reported for flexible-joint robotic manipulators with full state constraints. Likewise, a time-varying output constrained control was addressed for robotic manipulator on the basis of adaptive neural backstepping method [19]. Furthermore, an adaptive backstepping fixed-time control was constructed for MIMO systems, with a focus on the robotic manipulator subject to the output constraints [20]. Similarly, an adaptive finite-time control based on the backstepping method was proposed for robotic manipulators with funnel boundary [21]. Although [18]-[21] can be considered as the recent backstepping-based studies on the robotic manipulators, the design structures were based on the torque control strategy (TCS), the same as other studies reported in [1]- [17]. In other words, the actuator dynamics were ignored in the control designs. As a result, there would seem to be some problems (such as sensing limits and long process time) with the practical implementation of the TCS [22]. Moreover, the TCS-based control suffers from computational burden since the highly coupled nonlinear model of robot manipulators is directly involved in the construction of the control signal. Another drawback of the aforesaid studies [18]-[21] is that it may be difficult to be implemented on a real industrial robot in practice due to the complexity of the adaptation mechanism.

To overcome the drawbacks caused by TCS, voltage control strategy (VCS) was introduced by Fateh [22] to control electrically-driven robotic manipulators; in this case, the robot control problem was converted into the motor control problem with the aid of current feedback. The control law based on VCS is a model-free approach that also can be used in the high-speed tracking purposes for robotic manipulators. Several VCS-based control methods have been applied to robotic systems [23]-[26]. However, design of robust backstepping-based control using VCS is still an open issue for the robotic system. It is worth noting that even though some studies on the robotic manipulator have considered the motor dynamics in the modeling of the system, they have not followed the VCS since the manipulator dynamics were also involved in the control input, which made it more complex [27]-[30].

Inspired by the above discussions, this paper attempts to investigate the problem of adaptive voltage-based backstepping tracking control for uncertain robotic manipulators including actuator dynamics. First, a strict-feedback form of the integrated robotic system is proposed in the presence of external disturbances, un-modeled dynamics and parametric uncertainties. Then, two simple adaptation laws are obtained to compensate for lumped uncertainties in the framework of VCS. As a result, the proposed Lyapunov-based method has a robust behavior and the complexity of the control signal is reduced accordingly. Briefly, the contributions of the paper can be summarized as follows:

- Under external disturbances, un-modeled dynamics and parametric uncertainties, the model of robotic manipulator including actuator dynamics is presented in the form of an uncertain strict-feedback system.
- An adaptive robust voltage-based backstepping tracking controller is developed for electrically-driven robotic manipulators. To this end, two simple adaptive laws are obtained to compensate for the lumped uncertainties in the framework of VCS.
- With the aid of VCS, the practical restrictions of TCS are eliminated for the robotic system. Accordingly, the complexity of the control signal is reduced.
- Robust behavior, guaranteed stability and acceptable tracking error are the features of the proposed control law.

The rest of this paper is organized as follows: Section 2 presents the strict-feedback form of the electrically-driven robot manipulator. Section 3 introduces the proposed ARTB and the stability analysis is described in Section 4. Results and discussions are expressed in Section 5 in two subsections: first, the simulation results of ARTB are illustrated; then, three different backstepping-based controllers are simulated for comparison and the results are depicted. Finally, Section 6 concludes the paper.

II. MODELING

Deriving the strict feedback form of the robotic system is necessary for designing a suitable backstepping controller. All the equations are presented for a general n-DOF robot manipulator and a two-link manipulator including actuators is regarded as a case study. The manipulator dynamics is described [31] as

$$D(q)\ddot{q} + C(q.\dot{q})\dot{q} + G(q) = \tau \tag{1}$$

where $q, \dot{q} \in R^n$ and $\ddot{q} \in R^n$ are the joint positions, the vector of joint velocity and acceleration, respectively. $D(q) \in R^{n\times n}$ represents the inertia matrix, $C(q.\dot{q}) \epsilon R^{n\times n}$ is the Coriolis and Centrifugal torques, $G(q) \in R^n$ is the vector of gravitational torques and $\tau \in R^n$ represents the vector of the joint torque provided by electrical motors as follow

$$J_m\ddot{\theta}_m + B_m\dot{\theta}_m + r\tau = \tau_m \tag{2}$$

where J_m and B_m are the inertia and damping diagonal matrices for the motors. The motor torque (τ_m) is produced by the motor current (I_a) regarding the following equation as

$$\tau_m = K_m I_a \tag{3}$$

in which K_m is a diagonal constant matrix. The proportion of motor position vector (θ_m) to the joint position vector is introduced as

$$q = r\theta_m \;\rightarrow\; \theta_m = r^{-1}q \tag{4}$$

where $r \in R^{n*n}$ is the gear coefficient matrix. Substituting Equ. (3) and the derivatives of Equ. (4) up to the second order into Equ. (2) results in

$$\begin{aligned} &J_m r^{-1}\ddot{q} + B_m r^{-1}\dot{q} + r\tau = K_m I_a \;\rightarrow \\ &\ddot{q} = -J_m^{-1}B_m\dot{q} + rJ_m^{-1}K_m I_a - r^2 J_m^{-1}\tau \end{aligned} \tag{5}$$

The voltage of motors is considered as the control inputs. The electrical dynamic of motors is represented as

$$V = RI_a + L\dot{I}_a + k_b\dot{\theta}_m + \phi(t) + F(\dot{q}) \tag{6}$$

where k_b, R and L are $n \times n$ diagonal matrices for the back-emf constant, the resistance and inductance of motors, respectively. Moreover, $\phi(t)$ stands for external disturbances while the un-modeled dynamics are represented by $F(\dot{q})$. Equ. (6) can be written as

$$\begin{aligned} \dot{I}_a = L^{-1}V - L^{-1}RI_a - L^{-1}k_b r^{-1}\dot{q} - L^{-1}(\phi(t) \\ + F(\dot{q})) \end{aligned} \tag{7}$$

By defining the state vector as $X = (q, \dot{q}, I_a)^T$ and using Equs. (1), (5) and (7), the state-space model of the integrated robotic system is introduced as

$$\begin{aligned} \dot{x}_1 &= x_2 \\ \dot{x}_2 &= -J_m^{-1}B_m x_2 + rJ_m^{-1}K_m x_3 - r^2 J_m^{-1}(D(q)\ddot{q} \\ &\quad + C(q.\dot{q})\dot{q} + G(q)) \\ \dot{x}_3 &= -L^{-1}K_b r^{-1}x_2 - L^{-1}Rx_3 + L^{-1}V - L^{-1}(\phi(t) \\ &\quad + F(\dot{q})) \end{aligned} \tag{8}$$

For the sake of simplicity, Equ. (8) is formed as

$$\begin{aligned} \dot{x}_1 &= x_2 \\ \dot{x}_2 &= -a_1 x_2 + a_2 x_3 - r^2 J_m^{-1}(D(q)\ddot{q} + C(q.\dot{q})\dot{q} \\ &\quad + G(q)) \\ \dot{x}_3 &= -a_3 x_2 - a_4 x_3 + a_5 u - a_5(\phi(t) + F(\dot{q})) \end{aligned} \tag{9}$$

where

$$\begin{aligned} &a_1 = J_m^{-1}B_m \;,\; a_2 = rJ_m^{-1}K_m \;, a_3 = L^{-1}K_b r^{-1}, \\ &a_4 = L^{-1}R \;,\; a_5 = L^{-1} \end{aligned} \tag{10}$$

With respect to the nominal values of the weighted functions $(a_1, \dots, a_5)$, Equ. (9) can be expressed as

$$\begin{aligned} \dot{x}_1 &= x_2 \\ \dot{x}_2 &= -\hat{a}_1 x_2 + \hat{a}_2 x_3 + d_1 \\ \dot{x}_3 &= -\hat{a}_3 x_2 - \hat{a}_4 x_3 + \hat{a}_5 u + d_2 \end{aligned} \tag{11}$$

where $\hat{a}_1, \dots, \hat{a}_5$ are the nominal values and d_1 and d_2 are represented as

$$\begin{aligned} d_1 &= -r^2 J_m^{-1}(D(q)\ddot{q} + C(q.\dot{q})\dot{q} + G(q)) \\ &\quad + (\hat{a}_1 - a_1)x_2 - (\hat{a}_2 - a_2)x_3 \\ d_2 &= -a_5(\phi(t) + F(\dot{q})) + (\hat{a}_3 - a_3)x_2 \\ &\quad + (\hat{a}_4 - a_4)x_3 - (\hat{a}_5 - a_5)u \end{aligned} \tag{12}$$

The terms $D(q), G(q), C(q, \dot{q}), F(\dot{q}), \phi(t)$ and the differences between the real values and the nominal values of the weighted functions are included in the lumped uncertainties d_1 and d_2 as described by Equ. (12) and considered in the state space model Equ. (11). Note that $\hat{a}_i \,, i = 1, \dots, 5$ are known constant matrices, however $d_j \,, j = 1,2$ are unknown terms which are estimated via adaptation laws in the next section. Backstepping control is developed for Equ. (11) since it can be written in the form of strict feedback as follows:

$$\begin{aligned} \dot{\eta} &= f(\eta) + g(\eta)\zeta + d_1 \\ \dot{\zeta} &= f_a(\eta, \zeta) + g_a(\eta, \zeta)u + d_2 \end{aligned} \tag{13}$$

where

$$\begin{aligned} &\eta = \begin{pmatrix} x_1 \\ x_2 \end{pmatrix}, \zeta = x_3 \,, \\ &f(\eta) = \begin{pmatrix} x_2 \\ -\hat{a}_1 x_2 \end{pmatrix} \;,\; g(\eta) = \begin{pmatrix} 0 \\ \hat{a}_2 \end{pmatrix}, \\ &f_a(\eta, \zeta) = -\hat{a}_3 x_2 - \hat{a}_4 x_3 \,, \\ &g_a(\eta, \zeta) = \hat{a}_5 \end{aligned} \tag{14}$$

III. CONTROL DESIGN

In this section, a robust voltage controller based on backstepping method is designed for robot manipulator. The voltage-based controller obviates the complexity explosion of control effort and make the design too simple since the lumped uncertainties are compensated by two simple adaptation laws. More details and stability proof are given in what follows.

Step1) The position error is defined as

$$e_1 = x_1 - x_{1d} \tag{15}$$

where x_{1d} is the desired angle and e_1 represents the tracking error. The derivative of e_1 is defined as

$$\dot{e}_1 = \dot{x}_1 - \dot{x}_{1d} = x_2 - \dot{x}_{1d} = e_2 \tag{16}$$

For the first subsystem, the Lyapunov function is suggested as

$$V_1 = \frac{1}{2}e_1^T e_1 \tag{17}$$

Taking the derivative of V_1 results in

$$\dot{V}_1 = e_1^T \dot{e}_1 = e_1^T e_2 \tag{18}$$

while the virtual control signal is chosen as $e_2 = -\lambda_1 e_1$, the first subsystem become stable ($\dot{V}_1 = -e_1^T \lambda_1 e_1 \leq 0$).

Step2) We define z for the second subsystem as

$$z = e_2 + \lambda_1 e_1 \tag{19}$$

where λ_1 is a positive diagonal matrix. Using the second subsystem of Equ. (11), the derivative of Equ. (19) can be written as

$$\dot{z} = \dot{e}_2 + \lambda_1 \dot{e}_1 = (-\hat{a}_1 x_2 + \hat{a}_2 x_3 + d_1 - \ddot{x}_{1d}) + \lambda_1 z - \lambda_1^2 e_1 \quad (20)$$

The Lyapunov function is defined as

$$V_2 = V_1 + \frac{1}{2} z^T z + \frac{1}{2} \tilde{d}_1^T \gamma^{-1} \tilde{d}_1 \quad (21)$$

where $\tilde{d}_1 = d_1 - \hat{d}_1$. Thus, the derivative of V_2 is calculated as

$$\dot{V}_2 = \dot{V}_1 + z^T \dot{z} - \tilde{d}_1^T \gamma_1^{-1} \dot{\hat{d}}_1 \quad (22)$$

Substituting Equs. (18), (19) and (20) into Equ. (22) is written as

$$\dot{V}_2 = e_1^T (z - \lambda_1 e_1) + z^T (-\hat{a}_1 x_2 + \hat{a}_2 x_3 + d_1 - \ddot{x}_{1d} + \lambda_1 z - \lambda_1^2 e_1) - \tilde{d}_1^T \gamma_1^{-1} \dot{\hat{d}}_1 \quad (23)$$

Now by defining the $e_3 = x_3 - x_{3d}$, $\dot{V}_2$ is rewritten as

$$\dot{V}_2 = -e_1^T \lambda e_1 + e_1^T z - \tilde{d}_1^T \gamma_1^{-1} \dot{\hat{d}}_1 + z^T (-\hat{a}_1 x_2 + \hat{a}_2 e_3 + \hat{a}_2 x_{3d} + d_1 - \ddot{x}_{1d} + \lambda_1 z - \lambda_1^2 e_1) \quad (24)$$

x_{3d} is regarded as the virtual control input which can be chosen as

$$x_{3d} = (\hat{a}_2)^{-1} \left(\hat{a}_1 x_2 + \ddot{x}_{1d} - \lambda_1 z + \lambda_1^2 e_1 - e_1 - \lambda_2 z - \hat{d}_1 \right) \quad (25)$$

where λ_2 is a positive gain matrix. Substituting Equ. (25) into Equ. (24), the derivative of V_2 is simplified as

$$\dot{V}_2 = -e_1^T \lambda_1 e_1 - z^T \lambda_2 z + z^T \hat{a}_2 e_3 - \tilde{d}_1^T \left(z - \gamma_1^{-1} \dot{\hat{d}}_1 \right) \quad (26)$$

Thus, if the first adaptation law is chosen as $\dot{\hat{d}}_1 = \gamma_1 z$, ($\gamma_1$is a positive constant matrix) then $\dot{V}_2$ is obtained as

$$\dot{V}_2 = -e_1^T \lambda_1 e_1 - z^T \lambda_2 z + z^T \hat{a}_2 e_3 \quad (27)$$

Step3) Taking the derivative of e_3 and replacing the third subsystem of Equ. (11) yields

$$\dot{e}_3 = \dot{x}_3 - \dot{x}_{3d} = -\hat{a}_3 x_2 - \hat{a}_4 x_3 + \hat{a}_5 u + d_2 - \dot{x}_{3d} \quad (28)$$

The final positive definite Lyapunov function is introduced as

$$V_3 = V_2 + \frac{1}{2} e_3^T e_3 + \frac{1}{2} \tilde{d}_2^T \gamma_2^{-1} \tilde{d}_2 \quad (29)$$

Then, substituting Equ. (28) into the derivative of Equ. (29) results in

$$\dot{V}_3 = -e_1^T \lambda_1 e_1 - z^T \lambda_2 z + z^T \hat{a}_2 e_3 - \tilde{d}_2^T \gamma_2^{-1} \dot{\hat{d}}_2 + e_3^T (-\hat{a}_3 x_2 - \hat{a}_4 x_3 + \hat{a}_5 u + d_2 - \dot{x}_{3d}) \quad (30)$$

We choose the control input u in the following form

$$u = (\hat{a}_5)^{-1} \left[\hat{a}_4 x_3 + \hat{a}_3 x_2 - \hat{d}_2 + \dot{x}_{3d} - \lambda_3 e_3 - \hat{a}_2^T z \right] \quad (31)$$

where λ_3 is a positive gain and the second adaptation law is chosen as

$$\dot{\hat{d}}_2 = \gamma_2 e_3 \quad (32)$$

Finally, substituting Equ. (31) and Equ. (32) into Equ. (30) results in

$$\dot{V}_3 = -e_1^T \lambda_1 e_1 - z^T \lambda_2 z - e_3^T \lambda_3 e_3 \leq 0 \quad (33)$$

Therefore, the voltage control law Equ. (31) guarantees the stability of the closed-loop system. The Block diagram of the proposed controller is shown in Fig.1.

IV. Stability Analysis

Some assumptions are considered to verify the stability and well tracking of the proposed ARTB in the presence of uncertainties. It is worth noting that the assumptions are very common for nonlinear systems as clearly found in the literature.

Assumption 1: The desired trajectory q_d is required to be continuous and smooth such that its derivatives up to a necessary order are available and all uniformly bounded [23].

Assumption 2: The external disturbance $\phi(t)$ is bounded as $|\phi(t)| \leq \phi_{max}$ where ϕ_{max} is a positive constant [23].

Assumption 3: In general, the adaptation loop is processed with infinite operating frequency. Since the sampling interval is short enough as compared with the variation of d_1 and d_2, the lumped uncertainty terms are also assumed to be constant during estimation. As a result, the variations of the lumped uncertainties are considered to be zero in the adaptation process [32], [33].

Assumption 4: In order to protect the electrical motor against over voltage, we assume that the motor voltage is bounded as $|u(t)| \leq u_{max}$ [23], [25].

According to the previous section, the Lyapunov function is presented as

$$V_f = \frac{1}{2} e_1^T e_1 + \frac{1}{2} z^T z + \frac{1}{2} e_3^T e_3 + \frac{1}{2} \tilde{d}_2^T \gamma_2^{-1} \tilde{d}_2 + \frac{1}{2} \tilde{d}_2^T \gamma_2^{-1} \tilde{d}_2 \quad (34)$$

and the derivative of Equ. (34) results in

$$\dot{V}_f = -e_1^T \lambda_1 e_1 - z^T \lambda_2 z - e_3^T \lambda_3 e_3 \leq 0 \quad (35)$$

From Equ. (34) and Equ. (35), the boundedness of $e_1, z, e_3, \tilde{d}_1$ and $\tilde{d}_2$ are verified [34]. Based on the Assumption 1, q_d and $\dot{q}_d$ are bounded; hence boundedness of e_1 and z follows the boundedness of q and $\dot{q}$, respectively. The boundedness of I_a is depended on the boundedness of x_{3d} due to $I_a = x_3 = e_3 + x_{3d}$; From Equ. (25), x_{3d} is the virtual input composed of $\ddot{x}_{1d}, e_1, z$ and $\hat{d}_1$. According to the Assumption 3, d_1 is bounded. hence $\hat{d}_1$ is bounded with respect to the definition $\hat{d}_1 = d_1 - \tilde{d}_1$. Therefore, x_{3d} is bounded so the boundedness of I_a is confirmed. Moreover, the boundedness of $\hat{d}_2$ is proven similar to the boundedness of $\hat{d}_1$. Assumption 4 implies that the motor voltage is bounded, thus the proposed control

signal Equ. (31) is valid. So the guaranteed stability of the proposed ARTB is concluded.

V. Results And Discussions

Two subsections are considered to show the feasibility and effectiveness of the proposed controller. First, the proposed ARTB is applied to the uncertain electrically-driven robotic system and the results are presented; then, the second subsection is devoted to the comparison scenarios. The case study is a two-link robot manipulator driven by permanent magnet DC motors. The actuator specifications are presented in Table. 1 [35]. The desired trajectory for each joint is shown in Fig.2 since it is a smooth and differentiable path. As shown in Fig.3, the rectangular wave is an example of the external disturbance, similar to the one used in [25]. The ability of the proposed controller can be evaluated when facing the jumps in the external disturbance. In addition, $F(\dot{q})$ in (12) is also regarded as $0.1\dot{q}$ for the simulation. To consider the parametric uncertainties for the weighted functions, $\hat{a}_i$ is assumed to be 90% of the real value a_i.

A. Tracking Performance of the Proposed Controller

The proposed ARTB given by Equ. (31) is simulated with the following parameters:

$$\lambda_1 = \lambda_2 = \lambda_3 = 100 \times I_{2\times 2}, \quad \gamma_1 = [100\ 0; 0\ 500], \gamma_2 = 50 \times I_{2\times 2} \tag{36}$$

The satisfactory tracking performance of the proposed ARTB under the uncertainties is shown in Fig. 4. The four impulses in the zoomed mode of tracking performances are due to the four jumps in the profile of the external disturbance. It is shown that the jump times in Fig. 3 match the impulse times in Fig. 4(c) and (d). In addition, the impulses in the tracking performances are about 10^{-5} rad which are ignorable. As shown in Fig. 5, the behavior of the control inputs is smooth without the chattering problem. At first, the tracking error is high, so the controller injects high voltage into the system. Thus, the saturation is utilized to limit the voltage in the acceptable range. However, the input saturation influences for a short period in the control system. Afterwards, the range of voltages is permitted considering the type of motors. Hence, the effect of input saturation can be neglected after passing the transient state. Fig. 6 depicts the responses of d_1 and its estimation $\hat{d}_1$. It is demonstrated that the difference is ignorable. Likewise, d_2 and its estimation are given in Fig. 7, where $\hat{d}_2$ tracks d_2 as well. Therefore, the behavior of estimations is acceptable.

From this part of this study, it is concluded that the proposed control law succeeds in tracking the desired trajectory against uncertainties. In other words, the ARTB design is simple as well as more efficient since the complexity of control signal is eliminated by the voltage control strategy.

B. Comparison Scenarios

1) Example 1: State augmented adaptive backstepping control (SAAB)

First, it is worth noting that recent relevant papers on robotic systems have been developed based on the TCS, while the VCS has been rarely addressed in the literature, as clearly mentioned in this research. To this reason, the VCS is employed in this study. However, our control design is compared with three relevant papers applied to the robotic manipulators. The first scheme considered for the comparison is a state augmented adaptive backstepping (SAAB) control, adopted from [13]. To have a fair comparison, the model of robotic system is rewritten considering the motor dynamics. To this end, the final control law is obtained as

$$u = \phi\hat{\theta} + M\begin{pmatrix} k_p x_3 + k_i x_2 + n x_2 \\ +k_d\left(x_3 + k_p x_2 + \frac{k_i}{n} x_1\right)\end{pmatrix} \tag{37}$$

where k_p, k_i, k_d are positive constants. Variables x_1, x_2 and x_3 are also defined as $n\int_0^t e dt$, e and $\dot{e}$. The adaptation law is suggested as

$$\dot{\hat{\theta}} = \gamma\phi^T M^{-1}\left(x_3 + k_p x_2 + \frac{k_i}{n} x_1\right) \tag{38}$$

Vector ϕ is the regressor of the system derived from $M(q)\ddot{q}_d + H(q,\dot{q}) = \phi\theta$, where

$$M(q) = RK_m^{-1}J_m r^{-1} + RK_m^{-1} r D(q)$$
$$H(q,\dot{q}) = \begin{pmatrix} RK_m^{-1}B_m r^{-1} + K_b r^{-1} \\ +RK_m^{-1} r C(q,\dot{q})\end{pmatrix}\dot{q} + RK_m^{-1} r G(q) \tag{39}$$

The mathematical proof is omitted for brevity. More details of the design procedure can be found in [13]. The tuning parameters are chosen as $n = 5, k_p = 10, k_d = 5$ and $k_i = 0.1$. The tracking responses as well as tracking errors are shown in Fig. 8. The voltage of motors is depicted in Fig. 9. According to Figs. 8-9, the SAAB controller behaves well in tracking the desired trajectory with ignorable errors. However, the manipulator dynamics is involved in the control signal and adaptive law, which increases the complexity of design. In addition, the amplitude of the voltages is larger than our proposed method, in which some limitations may exist in practice with regard to the type of motors.

2) Example 2: Sliding mode-based adaptive backstepping design (SMAB)

To evaluate the strength of our proposed voltage-based controller, the control technique reported in [36] is also considered for the comparison. The actuator dynamics were included in the design procedure as addressed in the mentioned paper. The control input is provided as

$$u = RI_a + k_b\dot{q} + LH^{-1}f_2 - \rho z_2 \tag{40}$$

where the sliding surface s is defined as $\dot{q} - \dot{q}_d + K(q - q_d)$ and also z_2 and f_2 can be obtained through the backstepping method in the following form:

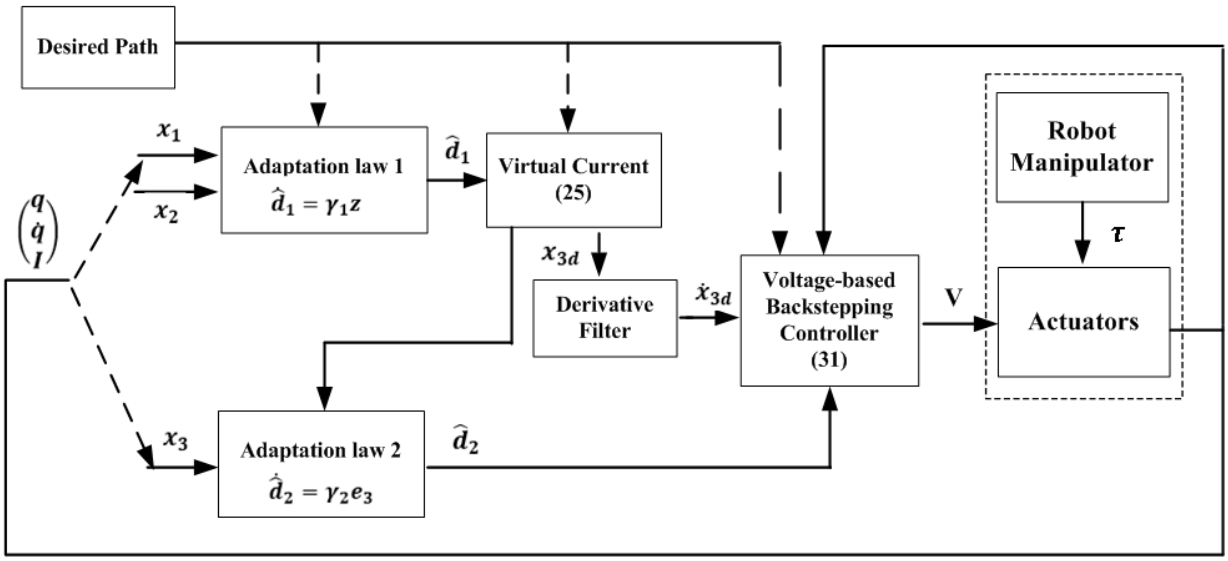


Fig. 1. The Block diagram of the proposed voltage-based backstepping control law (31)

TABLE I
SPECIFICATIONS OF DC MOTORS

Motors	u_{max} (v)	R (Ω)	J_m $(\frac{Nm.s^2}{rad})$	B_m $(\frac{Nm.s}{rad})$	L (H)	K_b $(\frac{V.s}{rad})$	r
1,2	50	1.6	0.0002	0.001	0.001	0.26	0.01

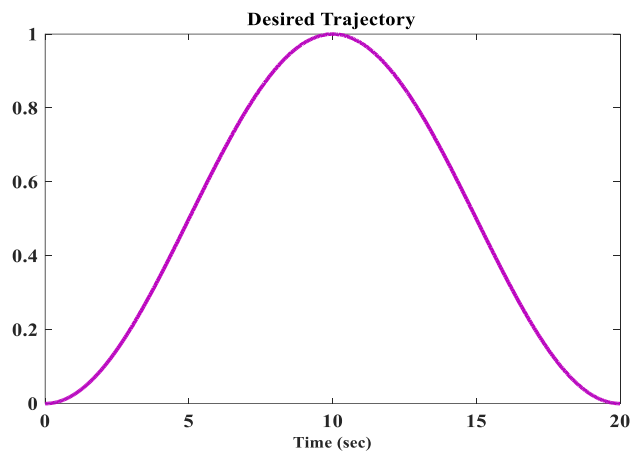


Fig. 2. The desired trajectory

$$z_2 = I_a - H^{-1}(Y\hat{\theta} - D(q)sat(\frac{S}{\epsilon})) \quad (41)$$

$$f_2 = \dot{Y}\hat{\theta} + Y\dot{\hat{\theta}} - \dot{D}(q)sat\left(\frac{S}{\epsilon}\right) - D(q)\dot{sat}\left(\frac{S}{\epsilon}\right) - HI_a + Y\hat{\theta} \quad (42)$$

in which the adaptive law is expressed as

$$\dot{\hat{\theta}} = -\Gamma(D^{-1}(q)s + H^{-1}z_2)Y \quad (43)$$

The tuning parameters are set to $K = 25 \times I_{2\times2}$, $\Gamma = 48 \times I_{2\times2}$ and $\rho = 100 \times I_{2\times2}$. More details were given in [36]. The initial conditions, the trajectory and the external disturbances are the same as the one used in our proposed method. As shown in Fig. 10, the tracking performance of SMAB is acceptable in the presence of uncertainties. The control inputs are located under the valid limited value as depicted in Fig. 11. However, the SMAB suffers from computational burden with respect to Equs. (40)-(43). In other words, the control effort has become more complex and difficult to be implemented on the industrial robotic manipulators.

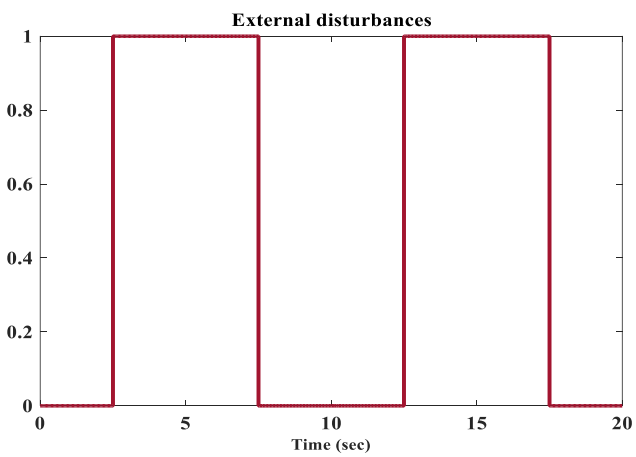


Fig. 3. The shape of external disturbance

3) Example 3: Adaptive backstepping sliding mode control (ABSM)

For comparison, an adaptive backstepping sliding mode control approach is also adopted from [37] and redesigned for the model of integrated robotic system. Similar to the previous subsections, all the simulation configuration (initial

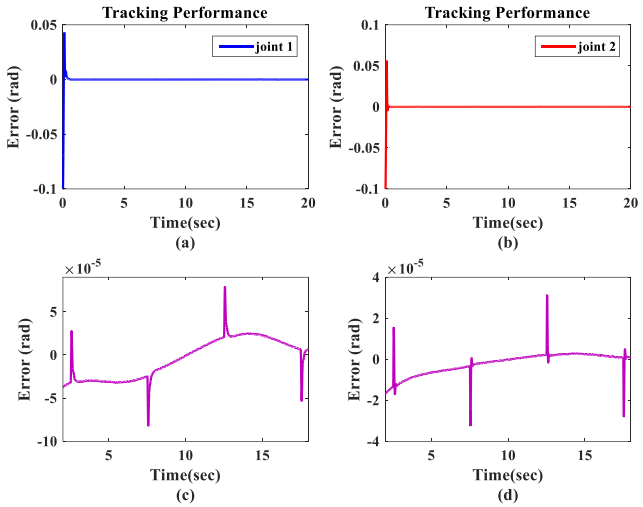


Fig. 4. (ARTB): (a) Tracking performance of first joint **(b)** Tracking performance of second joint **(c)** Zooming of (a) **(d)** Zooming of (b)

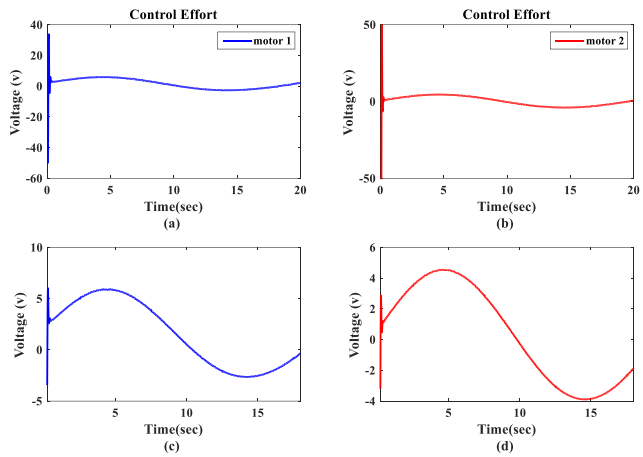


Fig. 5. (ARTB): (a) The control input of first joint **(b)** The control input of second joint **(c)** Zooming of (a) **(d)** Zooming of (b)

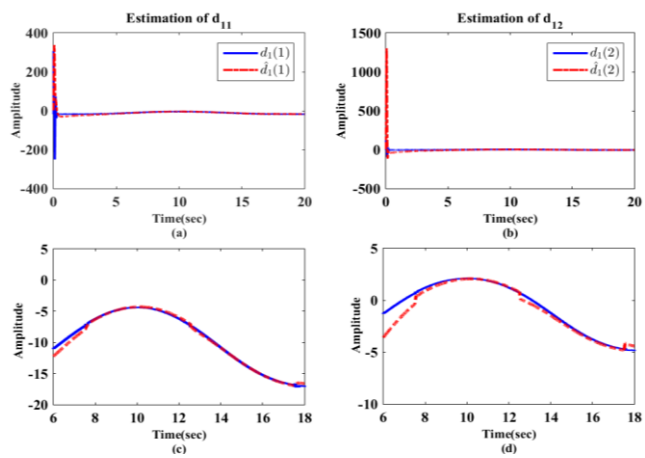


Fig. 6. Lumped Uncertainty Estimation 1: **(a)** d_{11} and $\hat{d}_{11}$ **(b)** d_{12} and $\hat{d}_{12}$ **(c)** Zooming of (a) **(d)** Zooming of (b)

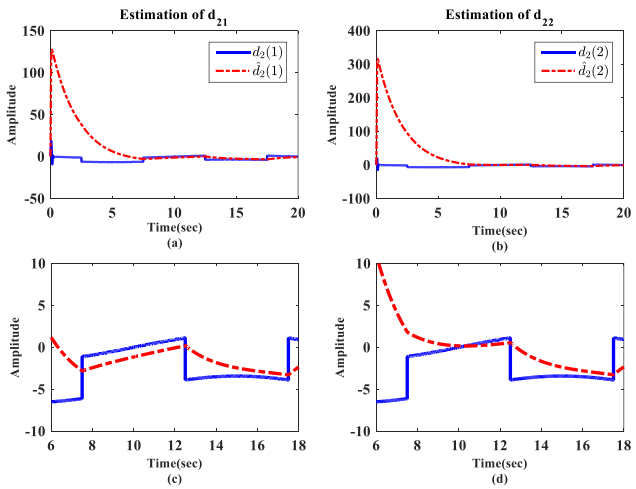


Fig. 7. Lumped Uncertainty Estimation 2: **(a)** d_{21} and $\hat{d}_{21}$**(b)** d_{22} and $\hat{d}_{22}$ **(c)** Zooming of (a) **(d)** Zooming of (b)

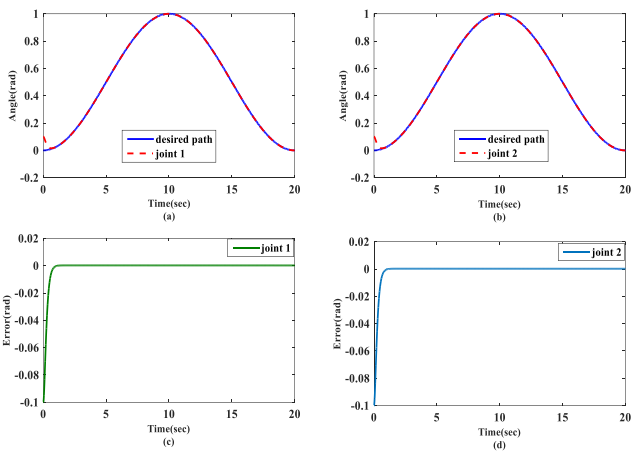


Fig. 8. Comparison 1: (SAAB) (a) Tracking response-first joint **(b)** Tracking response-second joint **(c)** Tracking error-first joint **(d)** Tracking error- second joint

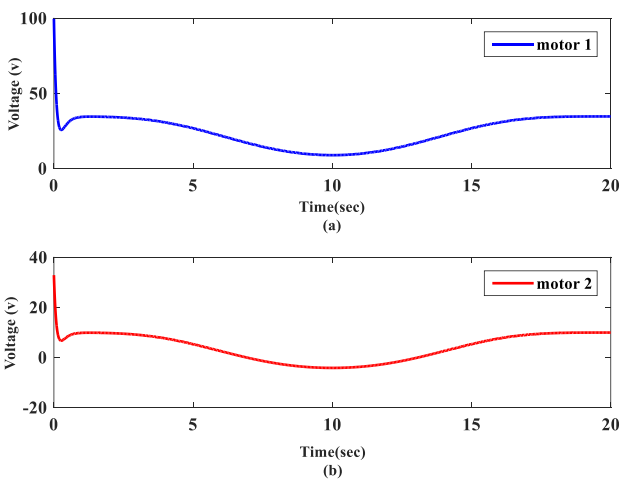


Fig. 9. Comparison 1: (SAAB) (a) Control input 1 **(b)** Control input 2

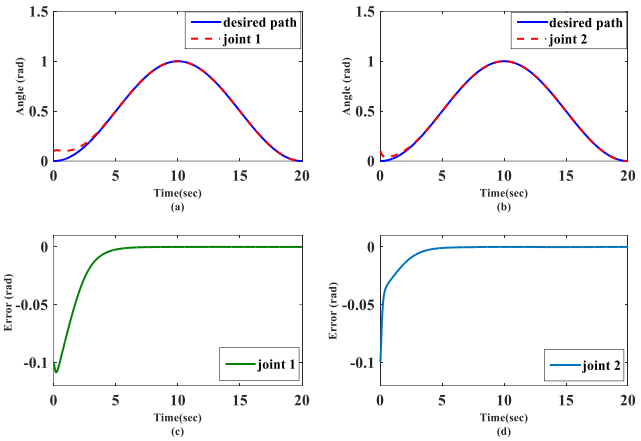


Fig. 10. Comparison 2: (SMAB) (a) Tracking response of first joint **(b)** Tracking response of second joint **(c)** Tracking error of first joint **(d)** Tracking error of second joint

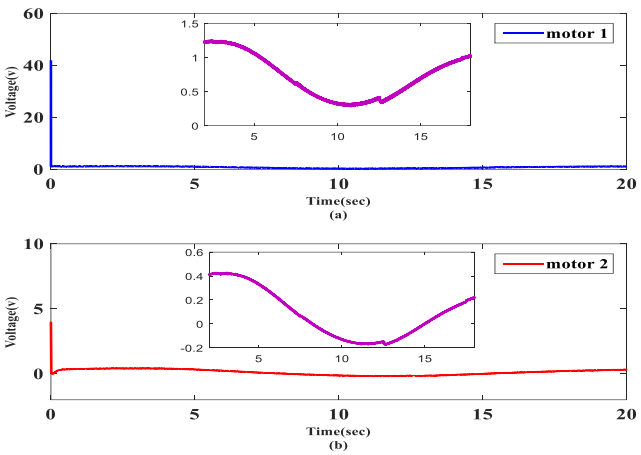


Fig. 11. Comparison 2: (SMAB) (a) Control effort of first joint **(b)** Control effort of second joint

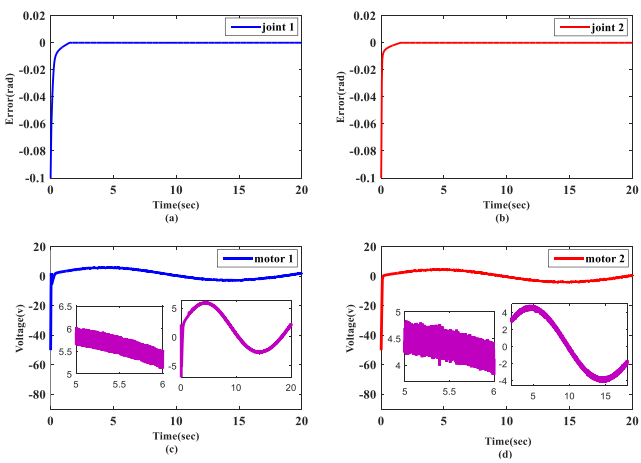


Fig. 12. Comparison 3: (ABSM) (a) Tracking error of first joint **(b)** Tracking error of second joint **(c)** Voltage of motor 1 **(d)** Voltage of motor 2

conditions, desired trajectory, external disturbance) are the same as one employed in the proposed ARTB controller. Therefore, the virtual input and the control input were derived as

$$x_{3d} = \hat{a}_2^{-1}(\hat{a}_1\dot{q} + \ddot{q}_d - k_1(\dot{q} - \dot{q}_d) - \lambda_1 s_1 - \gamma_1 sgn(s_1)) \tag{44}$$

$$u = \hat{a}_5^{-1}\big(\hat{a}_3\dot{q} + \hat{a}_4 I - \lambda_2 s_2 + \dot{I}_d - \hat{a}_2 s_1 - \gamma_2 sgn(s_2)\big) \tag{45}$$

in which $s_1 = (\dot{q} - \dot{q}_d) + k_1(q - q_d)$ and $s_2 = I_a - x_{3d}$. Furthermore, the upper bound of uncertainties can be obtained as

$$\dot{\gamma}_1 = \alpha_1\|s_1\|, \quad \dot{\gamma}_2 = \alpha_2\|s_2\| \tag{46}$$

The tuning parameters are chosen as $k_1 = 150 \times I_{2\times2}, \lambda_1 = 20 \times I_{2\times2}, \lambda_2 = 10 \times I_{2\times2}, \alpha_1 = diag(10{,}50)$ and $\alpha_2 = 2 \times I_{2\times2}$. Fig. 12(a)-(b) shows the tracking responses of ABSM controller. The voltage of motors is also exhibited in Fig. 12(c)-(d). Due to the existence of sign function in Equ. (44) and Equ. (45), the chattering phenomenon is appeared in the control inputs, which may damage to the actuators. To reduce the mentioned drawback, the saturation function can be used instead of sign function. However, it may lead to increase the tracking errors. Thus, a trade-off needs to considered between the stability and performance. It should be mentioned that our proposed method (ARTB) is relaxed from the aforesaid drawback.

To make a better comparison between the results of the control methods, we employ the performance criterion IAE (integral of absolute value of error), such that the superiority of the proposed ARTB to SAAB [13], SMAB [36] and ABSM [37] is shown in Table 2.

As a result, the main differences of the proposed controller ARTB with other methods can be listed as follows:

1) According to the IAE criterion, ARTB plays better performance in comparison with other methods.

2) ARTB is free from the manipulator dynamics while it is involved in SAAB and SMAB. Besides, our proposed adaptation mechanism is simpler than the laws described by (38) and (43).

3) ARTB is relaxed from the chattering phenomenon while ABSM suffers from it.

TABLE II
THE PERFORMANCE INDEX (IAE)

Control approach	*Joint 1*	*Joint 2*
The proposed ARTB	0.0082	0.0065
SAAB	0.0312	0.0102
SMAB	0.1988	0.0782
ABSM	0.0183	0.0094

VI. CONCLUSIONS

In this paper, an adaptive robust backstepping control law was proposed for the robot manipulator driven by electrical motors. First, a strict feedback form of the integrated robotic

system was presented and, then, the robust voltage-based controller was developed through the backstepping steps to facilitate the backstepping tracking problem for robotic systems. From the control point of view, the proposed method was effective since the heavily coupled nonlinear model of manipulator did not directly influence the design procedure and the suitable estimation of the manipulator dynamics was only utilized in the control scheme. Moreover, the performance of the proposed technique was satisfactory in terms of reducing the complexity of the control signal under uncertainties. Stability analysis guaranteed the boundedness of the closed-loop system using the Lyapunov function and acceptable tracking errors were satisfied by the simulation results. Finally, the comparison between the tracking performance of the ARTB and three recent relevant studies demonstrated the superiority of the proposed control technique.

REFERENCES

[1] M. Van, H.-J. Kang, and Y.-S. Suh, "Second Order Sliding Mode-Based Output Feedback Tracking Control for Uncertain Robot Manipulators," *Int. J. Adv. Robot. Syst.*, vol. 10, no. 1, pp. 1–9, 2013.

[2] Z. Zhang, L. Zheng, J. Yu, Y. Li, and Z. Yu, "Three Recurrent Neural Networks and Three Numerical Methods for Solving a Repetitive Motion Planning Scheme of Redundant Robot Manipulators," *IEEE/ASME Trans. Mechatronics*, vol. 22, no. 3, pp. 1423–1434, 2017.

[3] S. S. Saab and P. Ghanem, "A Multivariable Stochastic Tracking Controller for Robot Manipulators without Joint Velocities," *IEEE Trans. Automat. Contr.*, no. c, pp. 1–16, 2017.

[4] F. Sabahi, "Robot Action Space of Tractable Subsumption Architecture," *Int. J. Ind. Electron. Control Optim.*, vol. 2, no. 4, pp. 297–304, 2019.

[5] M. Vijay and D. Jena, "PSO based neuro fuzzy sliding mode control for a robot manipulator," *J. Electr. Syst. Inf. Technol.*, pp. 1–14, 2016.

[6] X. Yin and L. Pan, "Direct adaptive robust tracking control for 6 DOF industrial robot with enhanced accuracy," *ISA Trans.*, vol. 72, pp. 178–184, 2018.

[7] K. Yovchev, K. Delchev, and E. Krastev, "State Space Constrained Iterative Learning Control for Robotic Manipulators," *Asian J. Control*, vol. 20, no. 1, pp. 1–6, 2018.

[8] F. Bouakrif, "Trajectory tracking control using velocity observer and disturbances observer for uncertain robot manipulators without tachometers," *Meccanica*, vol. 52, no. 4–5, pp. 861–875, 2017.

[9] T. K. Roy, M. A. Mahmud, W. Shen, A. M. T. Oo, and M. E. Haque, "Robust nonlinear adaptive backstepping excitation controller design for rejecting external disturbances in multimachine power systems," *Int. J. Electr. Power Energy Syst.*, vol. 84, pp. 76–86, 2017.

[10] B. Xu, "Disturbance Observer-Based Dynamic Surface Control of Transport Aircraft With Continuous Heavy Cargo Airdrop," *IEEE Trans. Syst. Man Cybern. Syst.*, vol. 47, no. 1, pp. 161–170, 2017.

[11] W. Lv, F. Wang, and Y. Li, "Finite-time adaptive fuzzy output-feedback control of MIMO nonlinear systems with hysteresis," *Neurocomputing*, vol. 296, pp. 74–81, 2018.

[12] N. T. Binh, N. A. Tung, D. P. Nam, and N. H. Quang, "An Adaptive Backstepping Trajectory Tracking Control of a Tractor Trailer Wheeled Mobile Robot," *Int. J. Control. Autom. Syst.*, vol. 17, no. X, pp. 1–9, 2019.

[13] N. Nikdel, M. A. Badamchizadeh, V. Azimirad, and M. A. Nazari, "Adaptive backstepping control for an n-degree of freedom robotic manipulator based on combined state augmentation," *Robot. Comput. Integr. Manuf. Elsevier*, vol. 44, pp. 129–143, 2017.

[14] N. Nikdel, M. Badamchizadeh, V. Azimirad, and M. A. Nazari, "Fractional-Order Adaptive Backstepping Control of Robotic Manipulators in the Presence of Model Uncertainties and External Disturbances," *IEEE Trans. Ind. Electron.*, vol. 63, no. 10, pp. 6249–6256, 2016.

[15] S. I. Han and J. M. Lee, "Prescribed performance fuzzy backstepping control for nonlinear large-scale systems," *Int. J. Control. Autom. Syst.*, vol. 13, no. 6, pp. 1508–1520, 2015.

[16] A. Khajeh, F. Piltan, M. R. Rashidian, and A. Salehi, "Design New Intelligent PID like Fuzzy Backstepping Controller," *I.J Mod. Educ. Comput. Sci.*, vol. 2, no. February, pp. 15–26, 2014.

[17] M. Vijay and D. Jena, "Backstepping terminal sliding mode control of robot manipulator using radial basis functional neural networks," *Comput. Electr. Eng.*, pp. 1–18, 2017.

[18] W. Sun, S. F. Su, J. Xia, and V. T. Nguyen, "Adaptive Fuzzy Tracking Control of Flexible-Joint Robots With Full-State Constraints," *IEEE Trans. Syst. Man, Cybern. Syst.*, vol. PP, no. 99, pp. 1–9, 2018.

[19] Y. Wu, R. Huang, X. Li, and S. Liu, "Adaptive neural network control of uncertain robotic manipulators with external disturbance and time-varying output constraints," *Neurocomputing*, vol. 323, pp. 108–116, 2019.

[20] X. Jin, "Adaptive Fixed-Time Control for MIMO Nonlinear Systems with Asymmetric Output Constraints Using Universal Barrier Functions," *IEEE Trans. Automat. Contr.*, vol. 64, no. 7, pp. 3046–3053, 2019.

[21] J. Bao, H. Wang, and X. P. Liu, "Adaptive finite-time tracking control for robotic manipulators with funnel boundary," *Adapt. Control Signal Process.*, pp. 1–15, 2020.

[22] M. M. Fateh, "On the Voltage-based Control of Robot Manipulators," *Int. J. Control. Autom. Syst.*, vol. 6, no. 5, pp. 702–712, 2008.

[23] M. Souzanchi-K, A. Arab, M. R. T. Akbarzadeh, and M. M. Fateh, "Robust Impedance Control of Uncertain Mobile Manipulators Using Time-Delay Compensation," *IEEE Trans. Control Syst. Technol.*, vol. 26, no. 6, pp. 1943–1953, 2018.

[24] J. Keighobadi, M. M. Fateh, and H. Chenarani, "Adaptive fuzzy passivation control based on Backstepping Method for Electrically Driven Robotic Manipulators," *2018 6th RSI Int. Conf. Robot. Mechatronics*, no. IcRoM, pp. 292–297, 2018.

[25] M. M. Fateh and S. Fateh, "Decentralized direct adaptive fuzzy control of robots using voltage control strategy," *Nonlinear Dyn.*, vol. 70, no. 3, pp. 1919–1930,

2012.
[26] R. Gholipour and M. M. Fateh, “Adaptive task-space control of robot manipulators using the Fourier series expansion without task-space velocity measurements,” *Meas. J. Int. Meas. Confed.*, vol. 123, no. April, pp. 285–292, 2018.
[27] N. Nasiri, H. Sadjadian, and A. M. Shahri, “Voltage-based control of a flexible-joint electrically driven robot using backstepping approach,” *4th Annu. Int. Power Electron. Drive Syst. Technol. Conf.*, pp. 541–546, 2013.
[28] J. B. Mbede and J. J. B. Mvogo Ahanda, “Exponential Tracking Control Using Backstepping Approach for Voltage-Based Control of a Flexible Joint Electrically Driven Robot,” *J. Robot.*, pp. 1–11, 2014.
[29] C. Kwan and F. L. Lewis, “Robust backstepping control of nonlinear systems using neural networks,” *Syst. Man Cybern. Part A Syst. Humans, IEEE Trans.*, vol. 30, no. 6, pp. 753–766, 2000.
[30] S. E. Shafiei and M. R. Soltanpour, “Robust neural network control of electrically driven robot manipulator using backstepping approach,” *Int. J. Adv. Robot. Syst.*, vol. 6, no. 4, pp. 285–292, 2009.
[31] M. W. Spong, S. Hutchinson, and M. Vidyasagar, *Robot modeling and control*. New York, 2006.
[32] F.-J. Lin, S.-G. Chen, and I.-F. Sun, “Intelligent Sliding-Mode Position Control Using Recurrent Wavelet Fuzzy Neural Network for Electrical Power Steering System,” *Int. J. Fuzzy Syst.*, vol. 19, no. 5, pp. 1344–1361, 2017.
[33] F. J. Lin, C. K. Chang, and P. K. Huang, “FPGA-based adaptive backstepping sliding-mode control for linear induction motor drive,” *IEEE Trans. Power Electron.*, vol. 22, no. 4, pp. 1222–1231, 2007.
[34] J. E. Slotine and W. Li, *Applied Nonlinear Control*. Prentice-Hall, 1991.
[35] M. M. Zirkohi, M. M. Fateh, and M. A. Shoorehdeli, “Type-2 fuzzy control for a flexible-joint robot using voltage control strategy,” *Int. J. Autom. Comput.*, vol. 10, no. 3, pp. 242–255, 2013.
[36] Y. Hsiao, P. Tu, and J. Lin, “Sliding Backstepping Control Design for Robotic Manipulator Systems with Motor Dynamics,” *IEEE Int. Conf. Control Autom.*, pp. 667–672, 2014.
[37] M. A. M. Basri, “Design and application of an adaptive backstepping sliding mode controller for a six-DOF quadrotor aerial robot,” *Robotica*, vol. 36, no. 11, pp.1680-1700, 2018.



Javad Keighobadi was born in Sabzevar, Iran. He received the B.Sc. and M.Sc. degrees in Control engineering from Shahrood university of Technology, Iran in 2012 and 2014, respectively. He is currently working toward the Ph.D. degree at the Department of Electrical and Robotic Engineering, Shahrood University of Technology, Iran. His research interests include advanced nonlinear control, fuzzy learning control, robotics, and adaptive control.



Mohammad Mehdi Fateh received the B. Sc. degree from Isfahan University of Technology, Iran in 1988, the M. Sc. degree in electrical engineering from Tarbiat Modares University, Iran in 1991, and the Ph.D. degree from Southampton University, UK in 2001. He is a full professor at Department of Electrical and Robotic Engineering, Shahrood University of Technology, Iran. His research interests include nonlinear control, fuzzy control, robotics, intelligent systems, mechatronics and automation.